Effects of Process Parameters on Bondability in Thermosonic Copper Ball Bonding

Hui Xu[1], Changqing Liu[1], Vadim V. Silberschmidt[1], Honghui Wang[2]
[1]Wolfson School of Mechanical and Manufacturing Engineering, Loughborough University, Loughborough, LE11 3TU, UK
[2]Nantong Fujitsu Microelectronics co., Ltd, Jiangsu 226004, P. R. China
E-mail: H.Xu3@lboro.ac.uk, Phone: +44-1509-227684

Abstract

Thermosonic copper ball bonding is an absorbing interconnection technology that serves as a viable and cost saving alternative to gold ball bonding. Its excellent mechanical and electrical characteristics make copper ball bonding attractive for high-speed, power devices and fine-pitch applications. However, copper is easily oxidized and harder than gold, which causes some critical process problems in connection with bondability.

In this study, a 50 μm copper wire with purity of 99.99% was bonded on aluminum metallization with thickness 3 μm using an ASM angle 60 automatic thermosonic ball/wedge bonder. Experimental studies of copper free air balls (FABs) formation and bonding process were conducted to establish the bonding mechanism and to explain the effects of process parameters on bondability. A micro-slipping model was proposed to account for the effects of the ultrasonic power and bonding force on bondability. It was found that the bondability was determined by a slip area at the bonding interface. The occurrence of bonding only at the periphery of the contact area between FAB and aluminum metallization was attributed to partial slips at the bonding interface. Variation in the ultrasonic power and bonding force that lead to different stick-slip modes, can effect bondability in the ultrasonic bonding process. It is important to set a proper bonding time to achieve interatomic bonding without causing fatigue rupture of microjoints. It was also found that preheating of the chip to a certain temperature can improve bondability.

1. Introduction

Today, approximately 60 billion semiconductor, optoelectronic devices and micro-electro-mechanical systems (MEMS) are packaged annually; over 90% of these packages are implemented with thermosonic gold wire bonding due to the benefits of the process: self-cleaning, high yield rate, flexibility and reliability [1, 2]. With the miniaturization of the interconnection pitch and cost increase of the gold wire, thermosonic copper ball bonding, as an alternative technology for the most widely used gold ball bonding, is gaining more and more attention due to its excellent electronic, thermal and mechanical characteristics and low cost [3]. Nevertheless, copper ball bonding does come with its challenges. Copper oxidizes easily, so copper ball bonding must be performed in an inert atmosphere. In addition, copper is harder than gold and aluminum, which may lead to pushing metallization aside or even cratering on silicon chip. For these reasons, thermosonic copper ball bonding has not been broadly implemented in production, only accounting for a small portion, approx. 2%, of IC interconnections.

Ultrasound plays a key role in the bonding process. In the thermosonic/ultrasonic bonding process, the contamination and oxide layer can be broken down or removed by ultrasonic vibration at the interface [4]. In addition to this, based on the work by Langenecker [5], Harman [1] pointed out that an ultrasound energy can soften and heat materials, and then activate dislocations, reducing energy required to move them. Langenecker had compared elongations in aluminum single crystals exposed to 20 kHz ultrasonic vibration at constant temperature to equivalent elongations resulted from heating. It was found that ultrasound or heat can independently cause similar deformations for a given stress. However, significant differences exist between the two types of excitation: the ultrasonic energy density required to produce deformation in aluminum is about 10^7 times less than is required for an equivalent deformation resulted from thermal energy alone. Besides, the history of the interfacial temperature for bonds has been regarded as a good indicator to define the bonding process [6]. There have been some studies on measurement of interfacial temperature using liquid crystal and thermal sensors, but no accurate data was obtained so far due to a short bonding period and a small bonding region that is also opaque to non-invasive light probes. The footprints of ultrasonic aluminum wedge bonds on aluminum and copper metallization, studied by Harman and Albers [7], and Lum and Zhou [8], respectively, showed that the wire-to-pad microjoints were formed at points near the perimeter. But there are no reports of a lift-off pattern and footprint on copper bonds on aluminum metallization in literature.

Many efforts have been made to build a bonding model [9, 10]. A fretting mechanism was proposed by Hulst [11]. This theory supposed that interfacial sliding between the wire and pad cleaning and heating surface was a key factor for bonding. But it was not supported by measuring a movement of the wire during bonding. Measurements using a laser interferometer by Wilson et al. [12] indicated that the wire position remained fixed relative to the substrate, though capillary tool moved with an amplitude of 0.5-2.5 μm. Hence, a bond can be successfully made without interfacial motion. Therefore, the fretting, friction or sliding model became implausible. In addition, the sliding model predicted preferential bonding at the centre of the interface, while observations demonstrated that bonding occurred near the periphery and there was no bonding in a central zone [13]. Chen [14] pointed out that the most accepted explanation of the bond interface characteristics related to an elasticity model was proposed by Mindlin [15], though it

978-1-4244-2231-9/08/$25.00 ©2008 IEEE

was not specifically developed to account for wire bonding applications. Mindlin considered the contact between two spheres pressed into contact and analyzed the relative elastic displacements between the spheres under the action of oscillating tangential load. In the proposed model, the central region was referred to as elastic or non-slip region, while the outer area had been represented as exhibiting slip. But this explanation is only valid for very limited conditions because plastic deformation is common in the ultrasonic bonding process.

Some investigations [16-18] have been carried out to reveal the effects of process parameters. However, process optimization still remains a great technological challenge in copper ball bonding because of poor understanding of the mechanism of ultrasonic bonding. The importance of fundamental understanding of the effect of bonding parameters on bondability is evident by the continuing trend towards finer pitch bonding.

The objective of this work is to understand how process parameters affect the bond pattern and bondability in thermosonic copper ball bonding on an aluminum pad.

2. Experimental Procedures

Copper wire, supplied by SPM, with purity of 99.99%, 50 μm in diameter, elongation range of 20-30% and a break load range of 40-55 gf was chosen in this study. The copper FAB formation was carried out on an ASM angle 60 automatic thermosonic ball/wedge bonder. During a process, a high current was used to create high voltage to breach the inert gas gap, melting the tail of the copper wire to form a spherical ball. In order to prevent the oxidization of copper ball during FAB formation, a Copper Kit supplied by ASM was used. Forming gas ($95\%N_2/5\%H_2$) was used to provide an un-oxidizing atmosphere. The flow rate of the shielding gas was changed at several levels so as to obtain a high-quality copper FAB.

In this study, three criterions were defined to evaluate the quality of FAB, as follows:

(1) FAB characteristic dimension (size): D_A is the maximum diameter perpendicular to axis of the FAB whilst D_B is the distance between the end of FAB and boundary of wire and FAB, as seen in Figure 1. Then $(D_A+D_B)/2$ is defined as the FAB characteristic dimension. The FAB characteristic dimension is supposed to be optimum if it is twice the wire diameter.

(2) FAB shape tolerance: D_A/D_B is defined as the FAB shape tolerance, which is supposed to be optimum if it is close to 1.

(3) FAB surface condition: High quality of FAB is considered to be clean, metal-like, without voids and spots.

Dimensions and surface conduction of the FABs were recorded by JEOL JSM-5106LV scanning electronic microscopy.

A copper FAB was then performed on aluminum metallization to produce a bond. Four key factors (i.e. ultrasonic power, bonding force, bonding time, and initial temperature of preheated chip) determine the bonding process and affect the bond quality. Table 1 shows the levels of the bonding parameters for this experiment (1 gf = 9.8 mN). When one bonding parameter was changed in tests, other three

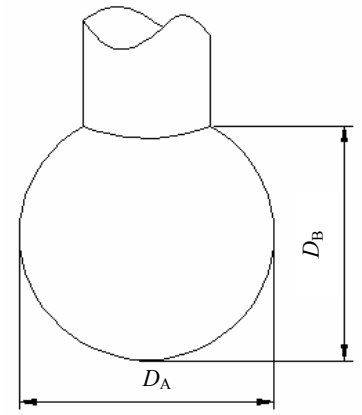

Figure 1 FAB geometry model

parameters were fixed. There were 28 runs in total, and 24 bonds were made for each set of parametric conditions. After bonding, the height and diameter of the mashed balls were recorded by Olympus STM6 optical microscopy and JEOL JSM-5106LV scanning electronic microscopy. The ball bonds were sheared in a DAGE 400 wire bond tester at 300 μm/s tool speed (shear rate), and 5 μm tool tip shear height. Both the geometry and shear test data were used to evaluate the quality of bonds in this study.

Table 1 Levels of the bonding parameters

Ultrasonic power (mW)	Bonding force (gf)	Bonding time (ms)	Initial temperature (°C)
60, 70, ***90***, 110, 130, 150,200	50, 80, ***110***, 140, 170, 200, 230, 260	2, 4, 8, 12, 20, ***28***, 36, 44, 60	25, 100, 140, 180, ***220***

Note: the bold and italic ones were used as the basic values of the bonding parameters.

3. Results and Discussion

3.1 Copper Ball Formation

The quality of FAB is vital to stability of the bonding process and quality of bonds. A pointed copper FAB, formed when the input energy is insufficient during electronic flame-off (EFO) process, would lead to cratering on a silicon chip (as shown in Figure 2) during subsequent bonding process, while a tilted FAB, shaped when the input energy is excessive or flow of shielding gas is too fast, could cause a golf bond (as shown in Figure 3). Both types of the defects could be avoided by optimizing the EFO parameters.

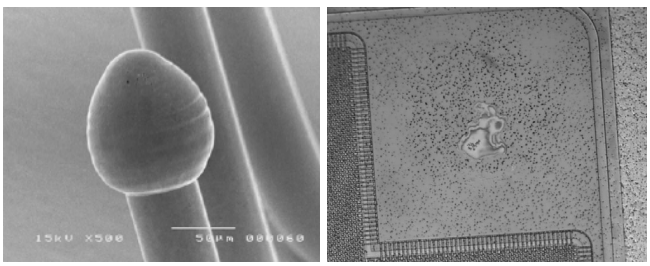

a) Pointed copper FAB b) Cratering on chip

Figure 2 Cratering caused by pointed FAB formed with insufficient input energy

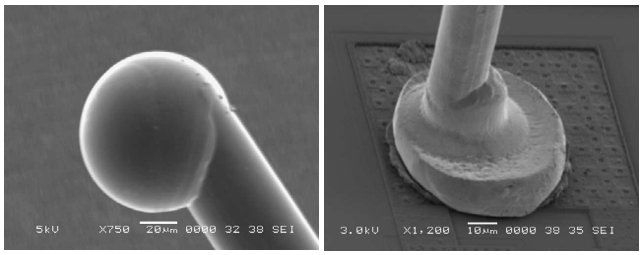

a) Tilted copper FAB b) Golf bond

Figure 3 Golf bond caused by tilted FAB formed with excessive input energy or too fast flow of shielding gas

In the gold ball formation process, the EFO current and fire time are the most significant factors [14]. In this study, these two parameters were optimized by design of experiment (DOE) (voltage was fixed at 5500 V by bonder system). A high-quality ball was formed with EFO current of 150 mA and fire time of 1300 µs which were then chosen for the following experiments.

It is supposed that the type of shielding gas used during the ball formation process plays an important role in FAB quality. If 100% purified nitrogen is used, it results in a total inert blanket and the cooling effect. However, the standard gas (i.e., $5\%H_2 95\%N_2$) could not only deplete oxygen to remove oxide that is present at the copper wire surface but also raise the heat energy to provide additional heat thermal energy to melt the copper wire by hydrogen gas. Thus, this forming gas was chosen as shielding gas for this study.

SEM images of copper FABs formed with and without shielding gas are given in Figure 4. It is clear that copper FABs formed without the shielding gas would be badly oxidized, with a rough surface, voids and oxide, and of a small size. Such FABs would not stick to the chip pad or lead-frame, while oxide-free, spherical FABs of a proper size were formed with the shielding gas, indicating that shielding gas would effectively protect copper from oxidization during the copper FAB formation process.

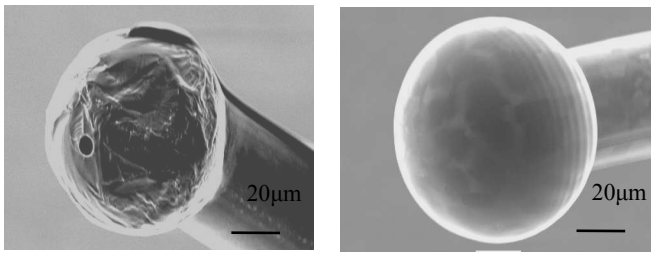

a) Without shielding gas
D_A:D_B : 70 µm : 61 µm

b) With shielding gas
D_A:D_B : 100 µm : 98 µm

Figure 4 SEM images of copper FABs formed with and without shielding gas

Figure 5 gives the SEM images of FABs for various flow rates of the shielding gas, ranging from 0.4 l/min to 1.6 l/min. The EFO currents and time were 150 mA and 1300 µs, respectively. When the gas flow speed is low, e.g. 0.4 l/min, the FAB would have an asymmetric shape with a point (as shown in Figure 5 a). This kind of the FAB trends to cause cratering on the silicon chip during the subsequent bonding process. If the flow rate is too high, the fielding gas would disturb the wire tail and make the FAB tilted during the EFO process. Therefore, both too low and too high flow rates have an adverse effect on FAB formation. Thus, a proper medium flow rate of shielding gas should be used, and 0.8-1.2 l/min is a preferable range used in this study.

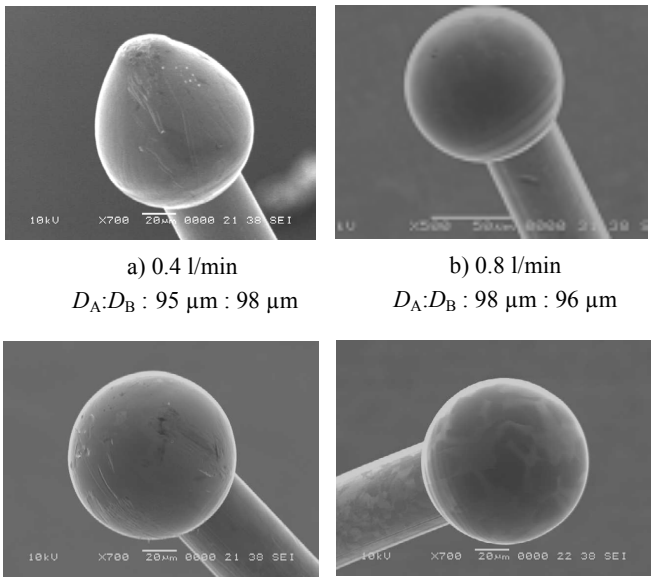

a) 0.4 l/min
D_A:D_B : 95 µm : 98 µm

b) 0.8 l/min
D_A:D_B : 98 µm : 96 µm

c) 1.2 l/min
D_A:D_B : 97 µm : 97 µm

d) 1.6 l/min
D_A:D_B µm : 96:94 µm

Figure 5 SEM images of copper FABs formed at different flow rates of shielding gas

It was surprising to see that when the forming gas was used, the copper FAB size with the shielding gas was larger than that in the still air. Moreover, the size of copper FABs increased with the growing forming gas flow rate up to 1.2 l/min. This is probably due to the additional heat provided by hydrogen. Higher gas flow rates decreased the FAB size due to the cooling effect of the shielding gas dominating at these conditions.\

3.2 Thermosonic Ball Bonding

3.2.1 Ultrasonic Power

The ultrasonic power is introduced by the transducer; it varied from 60 mW to 200 mW. Figure 6 shows the effects of ultrasonic power on the dimension of mashed copper ball when the bonding force, bonding time and initial temperature of preheated chip were fixed. The mashed ball is height decreased and its diameter increases steadily with the increase in the ultrasonic power. It suggests the ultrasound effectively softens materials, and makes it easier to deform them under the applied bonding force. The higher the ultrasound power, the more effective is softening. It is also obvious that the contact area grows more quickly when the ultrasonic power is higher than 150 mW.

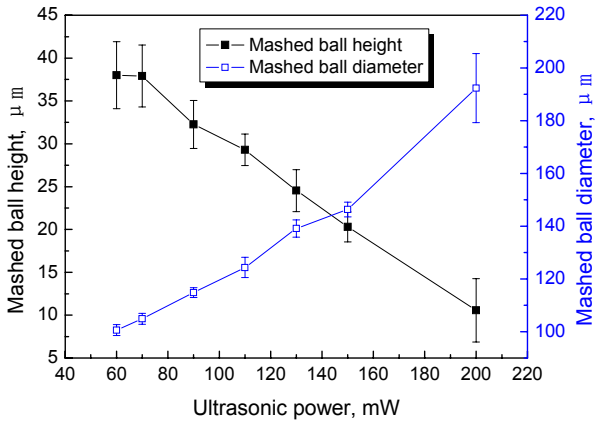

Figure 6 The effects of ultrasonic power on height and diameter of mashed copper ball. The bonding force, bonding time and initial temperature of preheated chip were fixed at 110 gf, 28 ms, and 220 °C, respectively.

The effects of ultrasonic power on shear force and strength of mashed copper ball is given in Figure 7. As the ultrasonic power increases, the ball shear force increases till it reaches a peak of 185 gf, then it decreases quickly. Shear strength is an indicator of bond interface properties rather than the shear force [19]. It was obtained by dividing the shear force by the area defined by the diameter of the deformed ball. The value of shear strength increases with ultrasonic power below 90 mW, since the shear force increases quickly but the contact area changes relatively slow at this range. Then, the shear strength remains constant at a high level. When the ultrasonic power is over 150 mW, the shear strength decreases dramatically due to the quick fall of the shear force and the growth of the contact area.

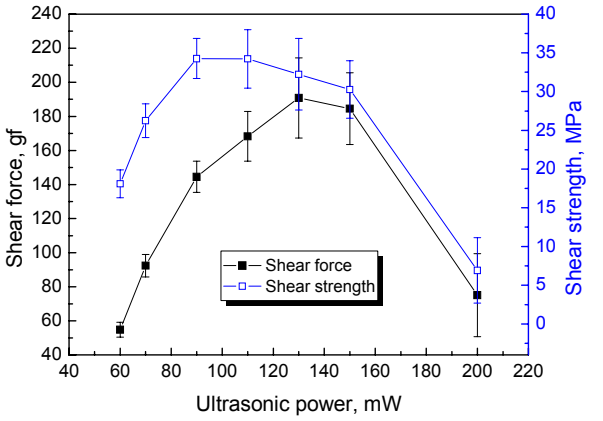

Figure 7 The effects of ultrasonic power on shear force and strength of mashed copper ball. The bonding force, bonding time and initial temperature of preheated chip were fixed at 110 gf, 28 ms, and 220 °C, respectively.

Clean metallic surfaces have high surface energies and make strong metallic bonds when in contact [20]. However, direct contact of fresh, clean surfaces is generally shielded by contamination and the oxide layer. Hence, contamination and the oxide layer at the contact interface is an important factor to be considered in determining the effects of the parameters on bondability. In the ultrasonic bonding process, contamination and the oxide layer will be broken down or removed by ultrasonic vibration at the interface. Therefore, the ultrasonic ball bonding process in the study can be roughly divided into three main stages. The first stage involves the removal of the contamination and the oxide layer covering the interface between the mashed copper ball and the pad. Secondly, as contamination and the oxide layer is broken down or removed, the underlying fresh metal surfaces are brought into contact under a normal force. Thirdly, interatomic forces come into action and atomic bonding occurs. Intermetallic or interdiffusion processes, if there are any, also occur at this stage. Moreover, according to the Mindlin's microslip theory, the slip area - and not the entire contact area - at the interface plays a crucial role in defining bondability.

As friction do not happen over the entire interface, only oxide and contaminants in the microslip area can be removed by ultrasonic vibration. So a lower ultrasonic power means a smaller microslip area and subsequently, less effective oxide and contaminants removal, leading to a non-stick on pad (NSOP). In this study, it was found that 60 mW was the least value needed for a successful bond. The value of the shear force increases with ultrasonic power, due to the increase in the microslip area. Figure 8 shows a typical bond with the wire bonded at the periphery of the contact area while the central area is left unbonded.

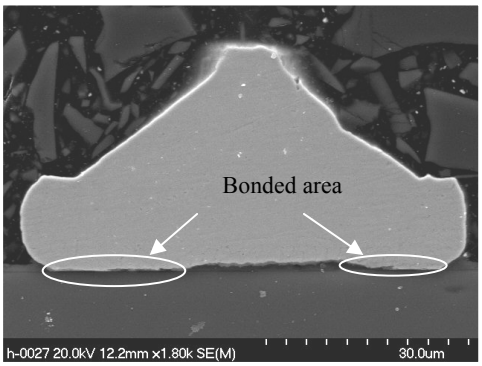

Figure 8 Copper bond with the wire bonded at the periphery and the central area unbonded

When ultrasonic excitation reaches a critical value, the entire contact area moves. In this case, an increase in the ultrasonic power will not lead to an increase in the shear strength. An excessive ultrasonic power could result in continuous rubbing during the whole bonding process, leaving insufficient time for interatomic or interdiffusion processes, thus causing poor bonding strength. In our experiments, it was found that the shear force decreased when the ultrasonic power was over 130 mW, and the shear force decreased when the ultrasonic power was over 90 mW.

In the electronic industry, the shear force and shear strength are commonly used as criterion for the quality evaluation of the bond, but other factors, such as mashed ball size, cratering and cracks on silicon chips should be also taken into account. A higher ultrasonic power always results in a greater extent of cratering to the chip, so a relatively low ultrasonic power is commonly adopted. So,

the ultrasonic power of 90 mW was chosen as a optimized parameter in our study.

3.2.2 Bonding Force

In our experiments, the bonding force varied from 50 gf to 260 gf. Results for the height and diameter of mashed copper ball with bonding force are shown in Figure 9 when the ultrasonic power, bonding time and Initial temperatures of preheated chip were fixed. The ball height decreases and diameter increases when the bonding force varies in its low range. Then value for the mashed ball is geometry remained almost constant for the bonding force between 110 gf and 170 gf. When bonding force continues to increase, the ball height decreases and the ball diameter increases again.

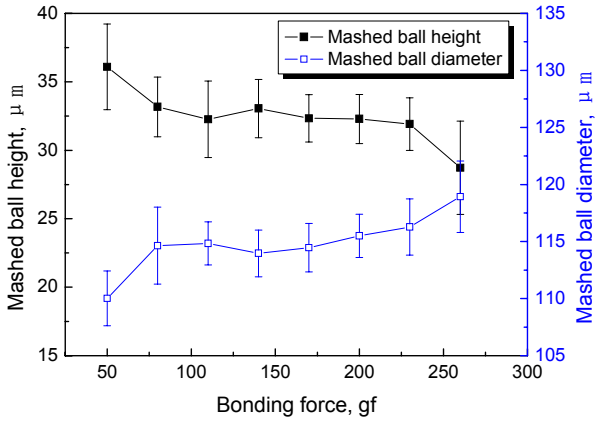

Figure 9 The effects of bonding force on height and diameter of mashed copper ball. The ultrasonic power, bonding time and Initial temperatures of preheated chip were fixed at 90 mW, 28 ms, 220°C, respectively.

The effects of the bonding force on the shear and strength of mashed copper ball is given in Figure 10. As the bonding force increases, the shear force increases at first, then remains constant, and decreases in the end. The maximum value is observed around 145 gf. The trend for the shear strength with bonding force is similar to that of the shear force. The maximum shear strength is about 35 MPa when the bonding force is between 110 gf and 170 gf.

As the applied normal force increases, the deformation of the ball changes from elastic to plastic, and the contact area increases. The evolution of the microslip region or the entire slip with the bonding force is similar to that in the case of tang ential force determined by the ultrasonic power. Up to a certain value of the bonding force, the entire slip always takes place. Before this certain value, the bonding strength increases with an increase in the bonding force. Thus, for effective oxide removing scrubbing, sufficient contact pressure is needed. The lower the bonding force, the less capillary-induced shear stress is available, resulting in a loose contact.

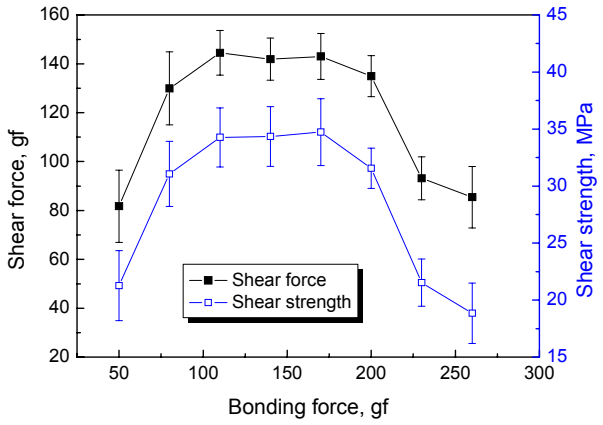

Figure 10 The effects of bonding force on shear force and strength of mashed copper ball. The ultrasonic power, bonding time and Initial temperatures of preheated chip were fixed at 90 mW, 28 ms, 220°C, respectively.

In the higher range of the bonding force, due to the constraint effect of friction on flow of the copper ball, the tangential traction in centre is lower than that at the periphery and the normal pressure at the interface will be higher in the centre than at the periphery. Thus, a relative motion in the central area will be constrained and, accordingly, there is no bonding. With an increasing bonding force, the central non-slip area increases. As a result of the competition between the increase in the contact area and the central non-slip area, the shear force does not change much for some range of the bonding force, then decreases with the increasing bonding force.

3.2.3 Bonding Time

The bonding time is the duration of ultrasound dissipation. In our tests, it varied between 2 ms and 60 ms. Resulting values for the mashed copper ball dimension with bonding time are shown in Figure 11 when the ultrasonic power, bonding force, and initial temperature of preheated chip remained constant. The mashed ball's height decreases and its diameter increases quickly at the first period (4 ms in this study) of the bonding process. This is due to the initial impact of the copper ball on the pad, causing large deformation. Then they remain nearly constant compared to a further rapid decrease of the ball height and an increase of the ball diameter for longer bonding times (44 ms and higher in this study). It suggests that ultrasonic softening takes place efficiently after a certain bonding time.

Experimental results of shear force and shear strength are shown in Figure 12. Whereas the shear force increases with bonding time until it reaches a constant value within reasonable bonding time, shear strength has a maximum value. In order to effectively remove oxide and contaminants, a sufficient bonding time is needed. Besides, too short a bonding time actives less time for an interatomic process. At the other extreme, an excessive bonding time produces an over grown mashed ball, decreasing bonding strength. Therefore an upper bonding time limit of 28 ms is chosen for the following experiments.

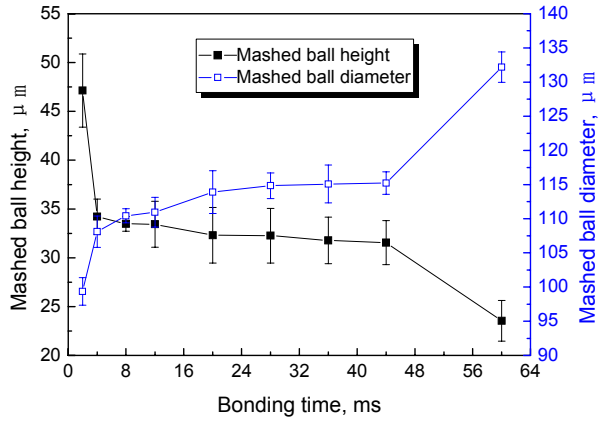

Figure 11 The effects of bonding time on height and diameter of mashed copper ball. Ultrasonic power, bonding force, and initial temperature of preheated chip were 90 mW, 110 gf, and 220°C, respectively.

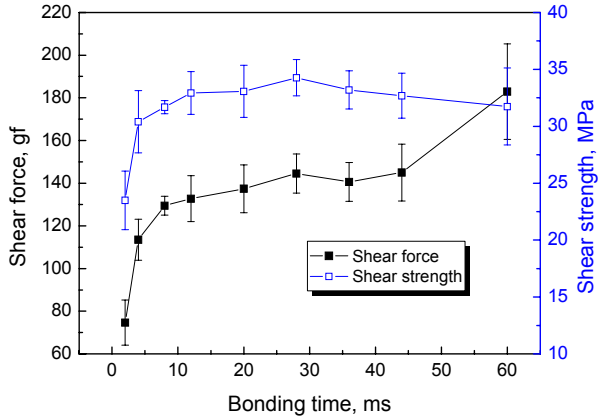

Figure 12 The effects of bonding time on shear force and strength of mashed copper ball. Ultrasonic power, bonding force, and initial temperature of preheated chip were 90 mW, 110 gf, and 220°C, respectively.

3.2.4 Initial Temperature

The initial temperature of preheated chip is the chip's temperature during bonding process conducted by the work holder. In our experiments, it ranged from 25 °C to 220 °C. Figure 13 presents the relationships between mashed ball's dimension and the initial temperature of preheated chip. With the initial temperature increasing, the height decreases and the diameter increases, but both change only slightly with the maximum height differences for the height 2 μm (approx. 6.0%) and diameter 6 μm (approx. 6.1%).

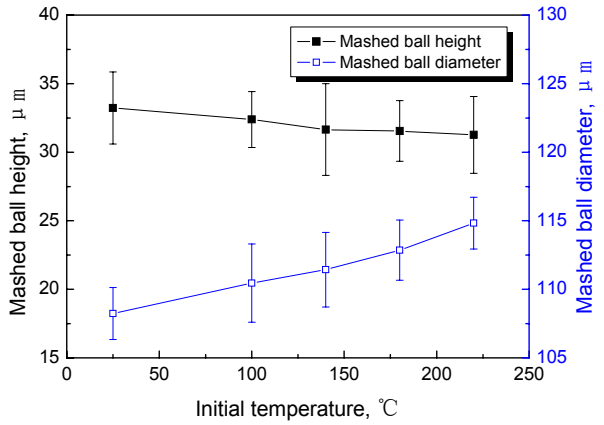

Figure 13 The effects of initial temperature of preheated chip on height and diameter of mashed copper ball. Ultrasonic power, bonding force, and bonding time were set at 90 mW, 110 gf, and 28 ms, respectively.

Unlike dimension of the mashed ball, the shear force and shear strength increase significantly with preheat temperature, as shown in Figure 14. Both shear force and shear strength raise monotonously, with peak values of 145 gf and 35 MPa, respectively, at 220 °C.

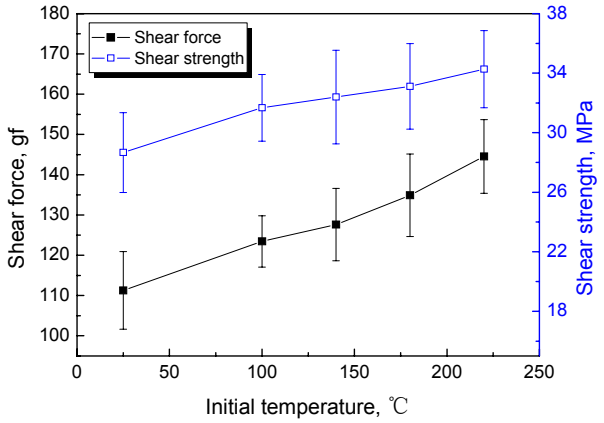

Figure 14 The effects of initial temperature of preheated chip on shear force and strength of mashed copper ball. Ultrasonic power, bonding force, and bonding time were set at 90 mW, 110 gf, and 28 ms, espectively.

The elevated temperature increases internal energy, improves atomic diffusion and solubility of the metals at the interface. Thus, the initial temperature of preheated chip, as a form of energy input, increases the bonding strength.

Conclusion

(1) Copper oxidization can be effectively prevented by shielding gas during the copper FAB formation process. The flow rate also affects the quality of copper FAB and was chosen between 0.8-1.2 l/min in this study for high quality.

(2) The effects of ultrasonic power, bonding force, bonding time and initial temperature on geometry of bonds and bonding strength were studied. A three-stage bonding model and a micro-slipping model were use to account for the effects of ultrasonic power and bonding force on

bondability. The bondability was determined by the slip area at the bonding interface. The transfer from the slip area to entire slip and visa versa was controlled by the levels of the ultrasonic power and bonding force, thus, these two parameters are the key factors affecting bondability. Furthermore, a proper bonding time was needed to support interatomic process, and the initial temperature of the preheated chip improved the atomic reaction.

Further work will focus on interface microstructure characterization of copper bonds by FIB and TEM so as to further ascertain the thermosonic bonding mechanism.

Acknowledgments

Authors would like to thank Mr Xiaochun Wu, leader of the technical section, and Mr Haiqing Zhu, an engineer in Fujitsu-NT Ltd. China, and Victoria Davis from CCLRC Rutherford Appleton Laboratory, UK, for their supports to this project.

References

1. Harman, G. G., Wire Bonding in Microelectronics, Materials, Processes, Reliability, and Yield. Second Edition. McGraw-Hill (New York; London, 1998).
2. Prasad, S. K., Advanced Wirebond Interconnection Technology, Springer (New York, 2004).
3. Valery, M. D., "Electrochemical Aspects of New Materials and Technologies in Microelectronics," *Microelectronic Engineering*, Vol. 70, No. 2 (2003), pp. 461-469.
4. Winchell, V. H. and Berg, H. M., "Enhancing Ultrasonic Bond Development," *IEEE Transactions on Components, Hybrids, and Manufacturing Technology*, Vol. 1, No. 3 (1978), pp. 211-219.
5. Langenecker, B., "Effect of Ultrasound on Deformation Characteristics of Metals," *IEEE Transactions on Sonics and Ultrasonics*, Vol. 13, No.1 (1966), pp. 1-8.
6. Panousis, N. T. *et al*, "Bonding Temperature Measurements during Device Assembly", *Solid State Technol,* , Vol. 26, No. 3 (1983), pp. 91-96.
7. Harman, G. G. and Albers, J., "The Ultrasonic Welding Mechanism as Applied to Aluminum and Gold Wire-Bonding in Microelectronics," *IEEE Transactions on Parts, Hybrids, and Packaging*, Vol. 13, No. 4 (1977), pp. 406-412.
8. Mayer, L. M. and Zhou, Y., "Footprint Study of Ultrasonic Wedge-bonding with Aluminum Wire on Copper Substrate," *Journal of Electronic Materials*, Vol. 35, No. 3 (2006), pp. 433-442.
9. Hu, C. M. *et al*, "A Microslip Model of the Bonding Process in Ultrasonic Wire Bonders Part I: Transient Response," *International Journal of Advanced Manufacturing Technolody*, Vol. 29, No. 9-10, (2006), pp. 860-866.
10. Hu, C. M. *et al*, "A Microslip Model of the Bonding Process in Ultrasonic Wire Bonders Part II: Steady State Response," *International Journal of Advanced Manufacturing Technolody*, Vol. 29, No. 11-12 (2006), pp. 1134-1142.
11. Hulst, A. P., "Ultrasonic Bonding of Insulated Wire," *Welding Journal*, Vol. 57, No. 2 (1978), pp. 19-25.
12. Wilson, A. D., "Holographic Interferometry Applied to Motion Studies of Ultrasonic Bonders," *IEEE Transation on Sonics and Ultrasonics*, Vol. 19, No.4 (1972), pp. 453-461.
13. Harman, G. G. and Albers J., "The Ultrasonic Welding Mechanism as Applied to Aluminum-and Gold-Wire Bonding in Microelectronics," *IEEE Transactions on Parts, Hybrids, and Packaging*, Vol. 14, No. 4 (1977), pp. 406-412.
14. Chen, G. K. C., "The Role of Micro-Slip in Ultrasonic Bonding of Microelectronic Dimensions," *International Hybrid Microelectronics Symposium*, 1972, 5A, pp. 111-119.
15. Mindlin, R. D. *et al*, "Effects of an Oscillating Tangential Force on the Contact Surfaces of Elastic Spheres," *Journal of Applied Mechanics-Transactions of the ASME*, Vol.18, No. 3 (1951), pp. 331-331.
16. Zhong, Z. W. *et al*, "Study of Factors Affecting the Hardness of Ball Bonds in Copper Wire Bonding," *Microelectronic Engineering*, Vol. 84, No. 2 (2007) 368–374.
17. Ding, Y. *et al*, "Effects of Bonding Force on Contact Pressure and Frictional Energy in Wire Bonding," *Microelectronics Reliability*, Vol. 46, No. 7 (2006), pp. 1101-1112.
18. Han, L. *et al*, "Bondability Window and Power Input for Wire Bonding," *Microelectronics Reliability*, Vol. 46, No.2-4 (2006), pp. 610-615.
19. Saraswati, *et al*, "High Temperature Storage (HTS) Performance of Copper Ball Bonding Wires," *Electronic Packaging Technology Conference*, Singapore, December. 2005, pp. 602-607.
20. Hong, S. J, *et al*, "The Behavior of FAB (Free Air Ball) and HAZ (Heat Affected Zone) in Fine Gold Wire," *International Symposium on Electronic Materials and Packaging*, South Korea, 2001, pp. 52-55.